Journal of Inorganic and General Chemistry
ZAAC
Zeitschrift für anorganische und allgemeine Chemie
DOI: 10.1002/zaac.202000142
ARTICLE

From a 1D Sb Coordination Polymer to a 3D Sb Framework with Pyrazine: Switching off the Stereochemically Active Lone-Pair

Jens R. Sorg,[a] Thomas C. Schäfer,[b] Tilman Schneider,[a] and Klaus Müller-Buschbaum*[a,b,c]

Dedicated to Prof. Dr. Hans-Jörg Deiseroth on the Occasion of his 75th Birthday

Abstract. The one-dimensional coordination polymer $^{1}_{\infty}[SbCl_3(pyz)]$ (**1**) and the three-dimensional frameworks $^{3}_{\infty}[Sb_2Cl_6(pyz)_3]$ (**2**) and $^{3}_{\infty}[Sb_2I_6(pyz)_3]$ (**3**) were obtained from SbX_3 (X: Cl, I) and pyrazine (pyz). These coordination polymers are, to the best of our knowledge, among the first Sb-based coordination polymers constructed from antimony halides and N-donor ligands. While the Sb^{3+}-cations in **1** are coordinated in a square-pyramidal coordination sphere indicating a stereochemically active lone-pair, no stereochemically active Sb-lone-pair is present in **2** and **3** having octahedral coordination spheres around Sb^{III}. Since **2** can be obtained by heating of **1**, the character of the Sb-lone-pair in **1** can be changed by thermal treatment. Thereby the interlinkage is increased via an additional pyrazine molecule resulting in the octahedral coordination in **2**.

Introduction

Antimony(III) complexes are known with various organic ligands,[1–10] such as 2,2′-bipyridine[1] or *N*,*N*′-disubstituted dithiomalonamides,[2] as well as antimony(V) complexes, e.g. for catecholates.[11–16] However, and to the best of our knowledge Sb^{III}-halide-based coordination polymers (CPs) constructed from N-donor ligands are just known from our recent work on $^{3}_{\infty}[Sb_2X_6(L)_2]$ and $^{1}_{\infty}[SbCl_3(bipy)]$ [X: Cl-I, L: 4,4'-bipyridine (bipy), 1,2-(4-pyridyl)ethylene (bpe), 1,2-(4-pyridyl)ethane (bpa)].[17] In the known complexes, the antimony atoms prefer octahedral (e.g. in $[Sb(L)_3]$, L: cyclohexylmetyl-, cyclohexylethyl-, cyclohexyldithio-carbamate)[18] or square pyramidal (e.g. $[Sb(PDC)(HPDC)(H_2O)]$)[19] coordination surroundings. The latter indicate stereochemically active Sb-lone-pairs repulsively interacting with the ligands.[20,21] The tendency of the lone-pair to be stereochemically active is thereby strongly influenced by the nature and orientation of the coordinating ligands.[22,23]

Coordination polymers (CPs), which are constructed from inorganic and organic building blocks by definition,[24] have proven to exhibit remarkable properties especially in terms of porosity (metal-organic-frameworks),[25–30] luminescence,[31–34] as well as catalytic applications.[35–39] Since the heavier homologue bismuth is known to form coordination polymers with remarkable luminescence properties,[40–47] antimony CPs can also be potentially attractive. Accordingly, we synthesized the compounds $^{1}_{\infty}[SbCl_3(pyz)]$ (**1**), $^{3}_{\infty}[Sb_2Cl_6(pyz)_3]$ (**2**), and $^{3}_{\infty}[Sb_2Cl_6(pyz)_3]$ (**3**) selecting the N-heterocycle pyrazine (pyz) that can serve as linear linker together with the halides SbX_3 (X: Cl, I). Pyrazine has proven to be a suitable ligand for such CPs in $^{2}_{\infty}[Bi_2Cl_6(pyz)_4]$,[48] which acts as host for luminescent Ln^{3+}-cations. Furthermore, formation of the CP $^{2}_{\infty}[BiI_3(pyz)]$ featuring structural similarities to the presented compounds has been reported recently.[49] The structural characteristics of the CPs **1–3** were studied and are discussed in this work, however, no luminescence could be observed for these compounds.

Results and Discussion

Crystal Structure

$^{1}_{\infty}[SbCl_3(pyz)]$ (**1**) crystallizes in the orthorhombic crystal system in the space group *Pbcm*. The one-dimensional CP is constructed from linear zigzag-chains, as shown in Figure 1. These chains contain $\{SbCl_3N_2\}$ square pyramids that are interconnected by pyrazine ligands, which are *cis*-oriented to one another. The apical position is occupied by one Cl atom with a short interatomic Sb–Cl distance [235.08(9) pm] compared to the basal Cl atoms [241.40(6) pm]. The interatomic Sb–N distance is 279.6(2) pm. The extended surrounding of the Sb atoms consists of three Cl atoms of neighboring strands with interatomic distances of 347.57(9) and 381.65(7) pm to the Sb atoms. As these distances are more than 100 pm larger than those for the apical and basal Cl atoms, it can be concluded

* Prof. Dr. K. Müller-Buschbaum
E-Mail: klaus.mueller-buschbaum@anorg.chemie.uni-giessen.de
[a] Institute of Inorganic Chemistry
Julius-Maximilians-Universität Würzburg
Am Hubland
97074 Würzburg, Germany
[b] Institute of Inorganic and Analytical Chemistry
Justus-Liebig-University Gießen
Heinrich-Buff-Ring 17
35392 Gießen, Germany
[c] Center for Materials Research (LAMA)
Justus-Liebig-University Giessen
Heinrich-Buff-Ring 16
35392 Giessen, Germany
Supporting information for this article is available on the WWW under **http://dx.doi.org/10.1002/zaac.202000142** or from the author.

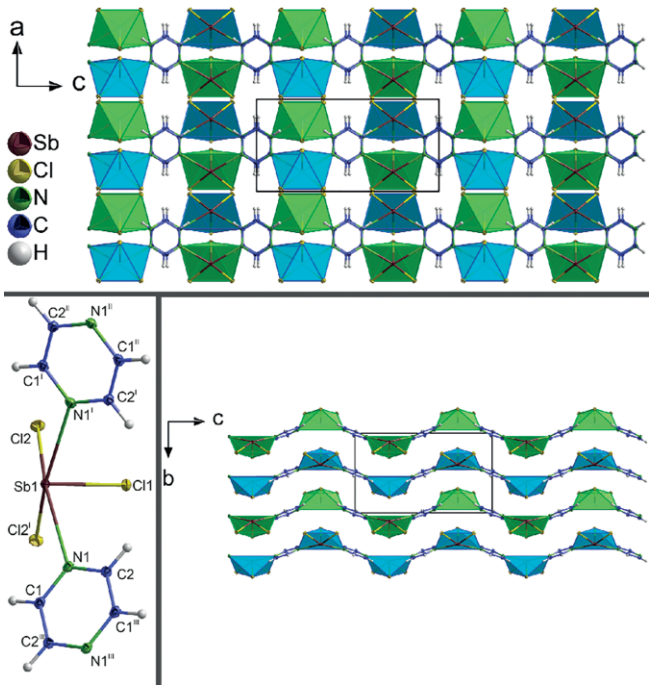

Figure 1. Top: crystal structure of $^{1}_{\infty}[SbCl_3(pyz)]$ (**1**) with a view along *b* axis; bottom left: extended coordination sphere of the Sb atoms in **1**; bottom right: crystal structure of **1** with a view along *a* axis. Symmetry code ^{i}: *x*, *y*, $^{3}/_{2}$ –*z*; ^{ii}: 1 –*x*, 1 –*y*, $^{1}/_{2}$ + *z*; ^{iii}: 1 –*x*, 1 –*y*, 1 –*z*. Ellipsoids represent a probability level of the atoms of 50 % in this and the following figures.

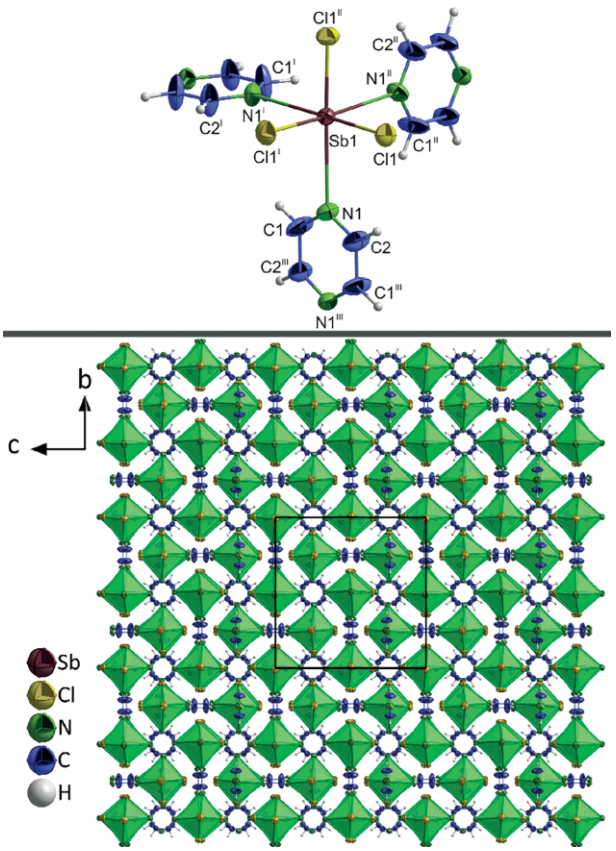

Figure 2. Top: extended coordination sphere of the Sb atoms in $^{3}_{\infty}[Sb_2Cl_6(pyz)_3]$ (**2**); bottom: crystal structure of **2** with a view along *a* axis. Symmetry code ^{i}: *y*, *z*, *x*; ^{ii}: *z*, *x*, *y*; ^{iii}: 1 –*x*, $^{1}/_{2}$ –*y*, *z*.

that the Sb-lone-pair interacts with the coordinating ligands stereochemically and thus, occupies the sixth corner of a pseudo-octahedral structure according to VSEPR (VSEPR: **v**alence **s**hell **e**lectron **p**air **r**epulsion).

The three-dimensional coordination polymer $^{3}_{\infty}[Sb_2Cl_6(pyz)_3]$ (**2**) crystallizes in the cubic crystal system in the space group $I\bar{4}3d$. The antimony atoms in this CP are octahedrally coordinated by three chlorido- and three pyrazine-ligands in a *fac* alignment with interatomic Sb–Cl and Sb–N distances of 240.08(14) and 281.6(5) pm, respectively (see Figure 2). The angles in the $\{SbCl_3N_3\}$-octahedra range from 84.09(1)° to 96.60(1)°. The distorted $\{SbCl_3N_3\}$ octahedra are interconnected by the pyrazine molecules in all three dimensions to form a dense framework structure. The distortion of the octahedra arises due to the different ligands rather than the Sb-lone-pair. Thus, no stereochemically active lone-pair is observed.

A closely related structure could be observed for $^{3}_{\infty}[Sb_2I_6(pyz)_3]$ (**3**). In contrast to **2**, this CP crystallizes in the trigonal crystal system in the space group *R*3*c*. Differences of the crystal structures of compounds **2** and **3** arise due to the differences in the interatomic Sb–X distances that are significantly elongated by approximately 40 pm by the replacement of Cl for I, while the Sb–N distances remain similar (see Table 1). Alike **2**, the crystal structure of **3** consists of distorted *fac*-$\{SbI_3N_3\}$ octahedra. The pyrazine-ligands interconnect these coordination units an all three spatial directions resulting in a dense three-dimensional coordination polymer. A depiction of the structure of **3** is given in Figure 3.

Table 1. Interatomic distances between the antimony atoms and the coordinating ligands in the coordination polymers **1**–**3**. Distances are given in pm.

	$^{1}_{\infty}[SbCl_3(pyz)]$ (**1**)	$^{3}_{\infty}[Sb_2Cl_6(pyz)_3]$ (**2**)	$^{3}_{\infty}[Sb_2I_6(pyz)_3]$ (**3**)
Sb–N	279.6(2)	281.6(5)	285.0(6)
Sb–X	Cl_{apical}: 235.08(9) Cl_{basal}: 241.40(6)	240.08(14)	277.96(6)

The interatomic distances between the antimony atoms and the coordinating ligands are given in Table 1. The Sb–X distances comply well with those of related compounds reported in the literature featuring Sb–Cl distances in the range of 240–319 pm[8,17,50] and Sb–I distances of 278–345 pm (X: I),[17,51] respectively. As these CPs are the first examples for Sb-based coordination polymers constructed from pyrazine, the interatomic Sb–N distances are of additional interest. Table 1 shows that they increase from Cl to I. However, the Sb–N distances reported for $^{1}_{\infty}[SbCl_3(bipy)]$[17] (bipy = 4,4′-bipyridine) as well as several complexes constructed from Sb-halides and 2-acetylpyridine-phenylhydrazone derivatives[8] or 1,10-phenanthroline,[9] in which the Sb^{3+}-cations feature square-pyramidal coordination spheres, are usually shorter (218–254 pm). This indicates comparatively weak Sb–N-interactions in **1**–**3** according to the rather low basicity of pyrazine and thus, low donor strength in comparison with other N-donor

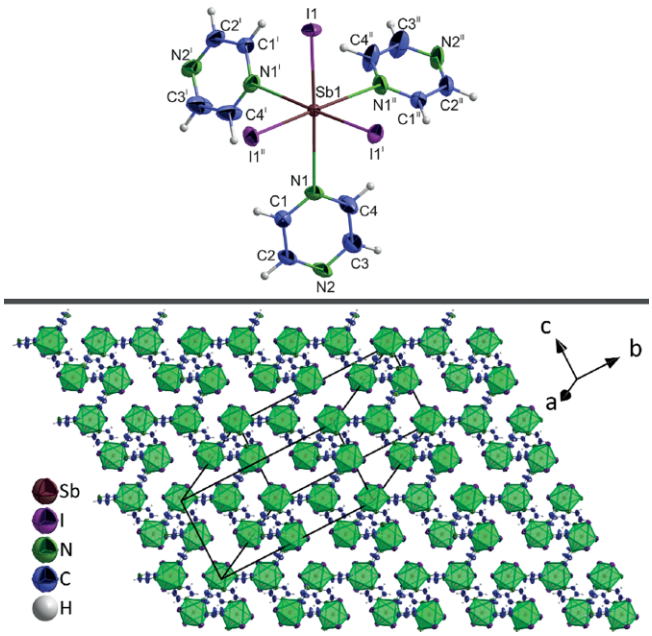

Figure 3. Top: extended coordination sphere of the Sb atoms in $^{3}_{\infty}[Sb_2I_6(pyz)_3]$ (**3**); bottom: crystal structure of **3**. Symmetry code ^{I}: $-x+y$, $1-x$, z; ^{II}: $1-y$, $1+x-y$, z;^{III}: $1-x$, $^{1}/_{2}-y$, z.

ligands, such as 1,10-phenanthrolin.[52,53] Interatomic distances of comparable magnitude were reported for 2,2′-bipyridine in $[Sb(CN)_3(2,2'\text{-bipy})]$ [$Sb–N_{2,2'-bipy}$: 256(1) pm, 272 pm] exhibiting long $Sb–N_{CN}$ distances of up to 341 pm.[54]

The bulk substances have been investigated with powder-X-ray-diffraction to prove the phase-purity of the coordination polymers. Thereby, a temperature-dependence in the lattice parameters of $^{1}_{\infty}[SbCl_3(pyz)]$ (**1**) was observed. Figure 4 (top) shows a comparison of the obtained diffractogram at room-temperature with simulated diffractograms from single-crystal-X-ray-diffraction data collected at 100 K and 300 K, respectively.

The change in the lattice parameters leads to differences in the reflection positions (marked with red asterisks in Figure 4), while the space-group *Pbcm* remains unchanged. The interatomic Sb–N distances at room temperature are elongated by 3.6 pm in comparison to those at 100 K, whereas the Sb–Cl distances are shortened by approximately 1.2 pm (cf. Figures S1–S3, Supporting Information). These changes lead to a non-uniform expansion of the unit cell [300 K: a' = 720.00(3) pm, b' = 841.31(4) pm, c' = 1426.61(6) pm; 100 K: a = 715.81(7) pm, b = 824.60(8) pm, c = 1418.34(15) pm] with b showing the largest increase [a'(300 K) = 1.006·a(100 K), b'(300 K) = 1.021·b(100 K), c'(300 K) = 1.006·c(100 K)] due to atomic vibrations at room temperature. This results in differently-sized shifts of the *hkl*-reflection positions towards lesser Bragg-angles, as the spacing of the lattice planes d_{hkl} in the orthorhombic crystal system, which affects the position of the reflections directly via Bragg's equation, is given by $d_{hkl} = 1/[(h/a)^2 + (k/b)^2 + (l/c)^2]$. Thus, reflections with a high value of the Miller-index k are shifted further than others resulting in an expansion of the separation of reflection positions, e.g.

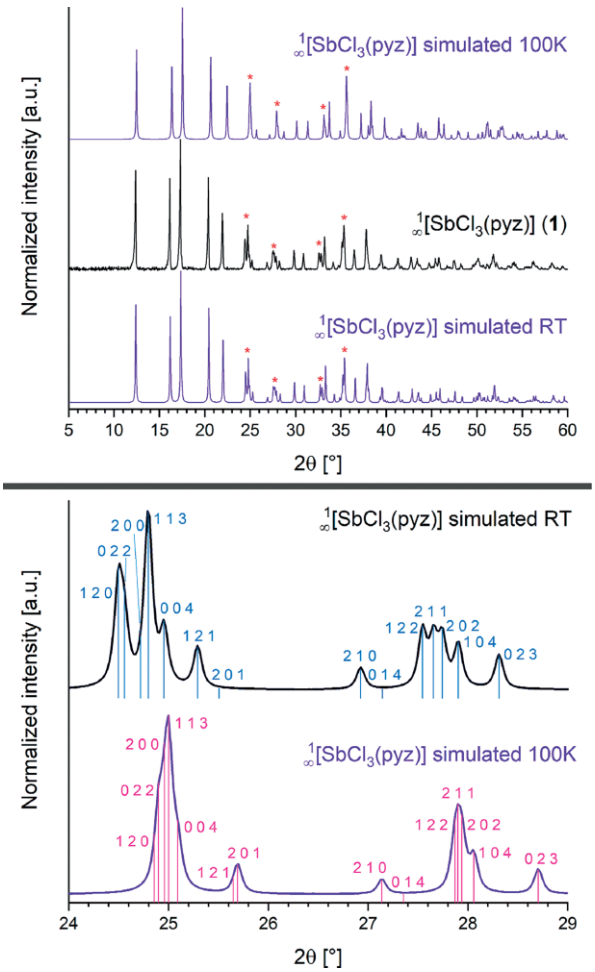

Figure 4. Top: Comparison of the obtained (black, middle) and diffractograms simulated from single-crystal-X-ray-diffraction data (violet) collected at 100 K (top) and 300 K (bottom) illustrating the phase-purity of $^{1}_{\infty}[SbCl_3(pyz)]$ (**1**). The red asterisks highlight the reflections featuring the most prominent differences. Bottom: Excerpts of the simulated powder diffractograms of $^{1}_{\infty}[SbCl_3(pyz)]$ (**1**) at 300 K (top, black) and 100 K (bottom, purple) with the respective *hkl* positions (blue, magenta) in the region $24°<2\theta<29°$ illustrating the cause of the reflection splitting in the obtained powder diffractogram of **1**.

around 25° and 28° in 2θ at 300 K from similar 2θ values at 100 K. Therefore, we ascribe this only ostensive "reflection-splitting" to overlapping *hkl*-reflection positions in the simulated diffractogram for 100 K, which are distinguishable from one another at room temperature because of the non-uniform unit cell expansion. To corroborate this explanation a detailed depiction of the simulated diffractograms at 100 K and RT in the region in which the reflection splitting is most prominent ($24°<2\theta<29°$) including the respective *hkl*-reflection positions is shown in the bottom part of Figure 4. Accordingly, the obtained diffractogram of **1** complies very well with the simulated one collected at room temperature and contains no additional reflections. Thus, the obtained bulk product of **1** can be considered phase-pure.

The obtained (RT) and simulated diffractograms (100 K) of $^{3}_{\infty}[Sb_2Cl_6(pyz)_3]$ (**2**) are depicted in Figure 5. They are in good accordance in terms of positions and intensities of the reflec-

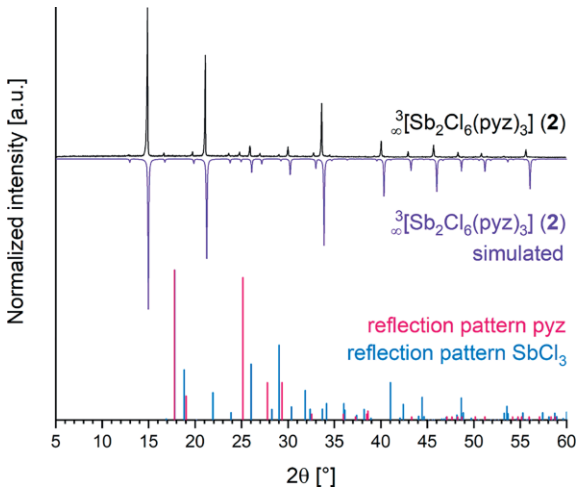

Figure 5. Comparison of the obtained (black) and the diffractogram simulated from single-crystal-X-ray-diffraction data collected at 100 K (violet), as well as reflection patterns of the reagents (magenta, blue) illustrating the phase-purity of $^{3}_{\infty}$[Sb$_2$Cl$_6$(pyz)$_3$] (**2**).

tions, only exhibiting the temperature related expansion of the unit cell at room temperature. No hints of excess reagents or other side-phases are observed for **2**.

In comparison, the halides of the heavier homologue bismuth form the two-dimensional CPs $^{2}_{\infty}$[Bi$_2$Cl$_6$(pyz)$_4$][48] and $^{2}_{\infty}$[BiI$_3$(pyz)][49] with pyrazine. While the coordination polymers **1**–**3** feature antimony coordination in square-pyramidal (**1**) or octahedral fashion (**2**, **3**), the bismuth atoms in $^{2}_{\infty}$[Bi$_2$Cl$_6$(pyz)$_4$][48] are surrounded by three pyrazine ligands and four chloride atoms in a capped trigonal prismatic coordination sphere. The crystal structure of $^{2}_{\infty}$[BiI$_3$(pyz)][49] contains bismuth atoms that are coordinated by four iodide atoms and two pyrazine molecules in an octahedral coordination sphere similar to that of $^{3}_{\infty}$[Sb$_2$X$_6$(pyz)$_3$] [X: Cl (**2**), I (**3**)], in which the antimony atoms are octahedrally coordinated by three pyrazine ligands and three halide atoms. Nonetheless, these crystal structures differ significantly in the interconnection of the coordination polyhedra. While they are interconnected in all three dimensions via pyrazine molecules in **2** and **3**, bridging iodide atoms lead to the formation of {Bi$_2$I$_6$N$_4$} double octahedra, which are linked by the pyrazine ligands to a two-dimensional structure in $^{2}_{\infty}$[BiI$_3$(pyz)].[49] Remarkably, decomposition of $^{2}_{\infty}$[BiI$_3$(pyz)][49] was reported during PXRD analyses resulting in the formation of a different crystalline phase. Comparable behavior could not be observed for the presented coordination polymers **1**–**3**, which are quite stable under X-ray radiation.

Synthesis

Since $^{1}_{\infty}$[SbCl$_3$(pyz)] (**1**) and $^{3}_{\infty}$[Sb$_2$Cl$_6$(pyz)$_3$] (**2**) can both be obtained from reactions of SbCl$_3$ and pyrazine, the reaction conditions conduct, which product is formed. Carrying out the reaction in a tetrahydrofuran (thf) solution at room temperature results in the formation of **1**. Reaction in the melt of the reagents gives one or the other compound depending on the reaction temperature. Thereby, milder temperatures favor the formation of **1**, whereas higher temperatures facilitate the formation of **2**. Increasing the temperature results in a higher linkage via pyrazine molecules.[55,56] Compound **2** is only formed above 100 °C and exclusively above 210 °C. In the temperature range of 100 °C to 210 °C a mixture of both CPs is obtained with the amount of **2** increasing with the temperature.

The framework **2** can also be obtained by thermal treatment of **1** at 210 °C. Thereby, **2** forms as colorless single-crystals together with the side product SbCl$_3$, which can be removed by sublimation in a second step. We investigated the transition from **1** into **2** with powder-x-ray-diffraction before and during the transition as well as differential scanning calorimetry (DSC). The obtained powder-diffractograms are shown in Figure 6 and verify the formation of **2**.

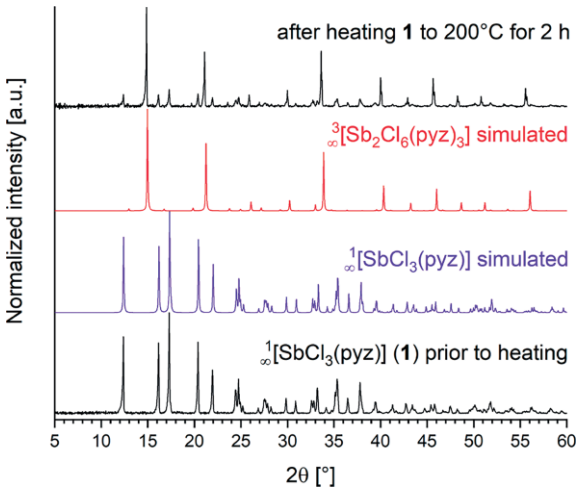

Figure 6. Comparison of the obtained (black) diffractograms of **1** prior (bottom) and subsequent to heating to 200 °C for 2 h (top) with the simulated diffractograms from single-crystal-X-ray-diffraction data of **1** (violet, middle) and **2** (red, middle) illustrating the thermal transition of $^{1}_{\infty}$[SbCl$_3$(pyz)] (**1**) into $^{3}_{\infty}$[Sb$_2$Cl$_6$(pyz)$_3$] (**2**).

While the diffractogram obtained prior to the thermal treatment only contains reflections of 1, the diffractogram after heating to 200 °C for two hours in a glass furnace contains a mixture of **1** and **2**, with **2** being the main phase. SbCl$_3$ formed as crystalline solid at the colder end of the ampoule and thus could be separated manually. The results of the DSC investigation of **1** are shown in Figure S4 (Supporting Information). The DSC heat flow contains a sharp endothermic signal with onset at 135 °C, which is followed by two additional broad endothermic signals between 170 and 210 °C. These signals represent the transition from **1** into **2** with subsequent sublimation of SbCl$_3$. The exothermic signals >220 °C can be assigned to decomposition processes.

$^{3}_{\infty}$[Sb$_2$I$_6$(pyz)$_3$] (**3**) is also accessible via a reaction in a self-consuming melt of the organic ligand at 100 °C. However, **3** is only formed as side-product in the reaction besides various unknown phases.

Conclusions

In this work, we present first examples of Sb-based coordination polymers constructed from SbX_3 (X: Cl, I) and pyrazine: a 1D strand $^1_\infty[SbCl_3(pyz)]$ (**1**) and the 3D frameworks $^3_\infty[Sb_2Cl_6(pyz)_3]$ (**2**) and $^3_\infty[Sb_2I_6(pyz)_3]$ (**3**). A stereochemically active lone-pair for antimony is observed in **1**, which leads to a square-pyramidal coordination of the Sb^{3+} cations. The character of the lone-pair can be changed by thermal conversion of the 1D- into a 3D-interlinked structure leading to the coordination and linkage of another pyrazine molecule to Sb^{3+} and thus, the formation of the 3D framework **2** from **1**. The crystal structures of **2** and **3** feature significant similarities, such as *fac*-$\{SbX_3N_3\}$ octahedra (X: Cl (**2**), I (**3**) as coordination units. Nonetheless, they crystallize in different crystal systems due to the change from Cl to I.

Experimental Section

All manipulations were carried out in inert atmospheric conditions using glovebox, ampoule, and vacuum line techniques. $SbCl_3$ (Sigma–Aldrich, 99.95 %), SbI_3 (abcr, 99.9 %) and pyrazine (Sigma–Aldrich, ≥ 99 %) were used as received.

Microanalyses were carried out on a Vario Micro Cube analyser. IR spectra were recorded with a THERMO Nicolet 380 FT-IR spectrometer in transmission mode using an ATR-unit (see Figure S5, Supporting Information, for IR spectra). DSC investigations were performed on a DSC 204 F1 Phoenix (Netzsch) in N_2 atmosphere with a heating rate of 10 K·min^{-1}.

X-ray Crystallography: Single crystal X-ray determinations were performed on a BRUKER AXS Smart Apex 1 diffractometer with graphite monochromator (Mo-K_α radiation; λ = 0.71073 Å) at 100 K (**1**, **2**), 200 K (**3**) or 300 K (**1**), respectively. The structures were solved by direct methods, refined with the least-squares method by ShelXL[57–59] and expanded using Fourier techniques, all within the OLEX2 software suite.[60] All non-hydrogen atoms were refined anisotropically. Hydrogen atoms were assigned to idealized geometric positions and included in structure factors calculations. Pictures of the crystal structures were created using DIAMOND.[61] Generally, interatomic distances are of expected values.

Crystallographic data (excluding structure factors) for the structures in this paper have been deposited with the Cambridge Crystallographic Data Centre, CCDC, 12 Union Road, Cambridge CB21EZ, UK. Copies of the data can be obtained free of charge on quoting the depository numbers CCDC-1970944, CCDC-1970945, CCDC-1970946, and CCDC-1970947 for **1**–**3** (Fax: +44-1223-336-033; E-Mail: deposit@ccdc.cam.ac.uk, http://www.ccdc.cam.ac.uk).

Crystal Data for $^1_\infty[SbCl_3(pyz)]$ (1): $SbCl_3C_4H_4N_2$ (M = 308.20 g·mol^{-1}, colorless): orthorhombic, space group *Pbcm* (no. 57), a = 715.81(7) pm, b = 824.60(8) pm, c = 1418.34(15) pm, V = 5.3649(19) × 10^9 pm^3, $\rho_{calcd.}$ = 2.445 g·cm^{-3}, T = 100 K, μ(Mo-K_α) = 4.177 mm^{-1}, 14597 reflections measured (5.692° ≤ 2Θ ≤ 58.642°), 1191 unique (R_{int} = 0.0634, R_{sigma} = 0.0278) which were used in all calculations. GOF: 1.057. Final R_1 = 0.0202 [$I > 2\sigma(I)$], wR_2 = 0.0387 (all data).

Crystal Data for $^3_\infty[Sb_2Cl_6(pyz)_3]$ (2): $SbCl_3C_6H_6N_3$ (M = 696.49 g·mol^{-1}, colorless): cubic, space group $I\bar{4}3d$ (no. 220), a = 16720(4) pm, V = 4.675(3) × 10^9 pm^3, $\rho_{calcd.}$ = 1.979 g cm^{-3}, T = 100 K, μ(Mo-K_α) = 3.007 mm^{-1}, 74959 reflections measured (5.968° ≤ 2Θ ≤ 61.574°), 1224 unique (R_{int} = 0.0974, R_{sigma} = 0.0177) which were used in all calculations. GOF: 1.025. Final R_1 = 0.0293 [$I > 2\sigma(I)$], wR_2 = 0.0619 (all data).

Crystal Data for $^3_\infty[Sb_2I_6(pyz)_3]$ (3): $SbI_3C_6H_6N_3$ (M = 1245.22 g·mol^{-1}, orange): trigonal, space group $R3c$ (no. 161), a = b = 2601.55(7) pm, c = 1401.80(4) pm, α = β = 90°, γ = 120°, V = 8.2164(5) × 10^9 pm^3, $\rho_{calcd.}$ = 3.020 g cm^{-3}, T = 100 K, μ(Mo-K_α) = 8.746 mm^{-1}, 73772 reflections measured (3.13° ≤ 2Θ ≤ 56.698°), 4568 unique (R_{int} = 0.0535, R_{sigma} = 0.0194) which were used in all calculations. GOF: 1.042. Final R_1 = 0.0203 [$I > 2\sigma(I)$], wR_2 = 0.0478 (all data).

PXRD analysis was carried out on a Bruker D8 Discover diffractometer with Da Vinci design, focusing Göbel mirror and linear LynxEye detector in a parallel beam geometry in transmission mode (**1**) and a STOE STADI P with focusing Ge(111) monochromator and MYTHEN 1 K strip detector (DECTRIS) in Debye–Scherrer setup (**2**). Powder samples were prepared in Lindemann glass capillaries with 0.5 mm diameter under inert gas atmosphere. The samples were measured using Cu-K_α radiation (λ = 1.54056 Å).

Synthesis of $^1_\infty[SbCl_3(pyz)]$ (1): Reaction of 57.0 mg $SbCl_3$ (1 equiv., 250 µmol) with 20.1 mg pyrazine (1 equiv., 250 µmol) in a solution of 5 mL tetrahydrofuran (thf) at room temperature leads to the formation of **1**. Therefore, both reagents were dissolved in 2.5 mL thf, each. Subsequently, the pyrazine solution was added dropwise to the $SbCl_3$ solution. **1** was formed instantly as colorless precipitate. The reaction was completed by additional stirring for 30 minutes. After filtration and subsequent drying in vacuo, **1** was obtained as colorless solid and characterized by single-crystal and powder-X-ray diffraction analyses as well as IR spectroscopy. $SbClC_4H_4N_2$: calcd. C: 15.59, H: 1.31, N: 9.09 %; found: C: 15.29, H: 1.38, N: 8.68 %. **FT-IR** (ATR): $\tilde{\nu}$ = 3128 (w), 3095 (w), 3059 (w), 2965 (w), 1602 (w), 1573 (w), 1508 (m), 1482 (m), 1408 (s), 1368 (m), 1309 (w), 1260 (m), 1173 (m), 1157(m), 1148 (m), 1124 (s), 1078 (m), 1057 (m), 1031 (s), 795 (s), 777 (m) cm^{-1}.

Synthesis of $^3_\infty[Sb_2Cl_6(pyz)_3]$ (2): 2 was obtained by a solvent-free melt reaction of 114.0 mg $SbCl_3$ (1 equiv., 500 µmol) with 120 mg pyrazine (3 equiv., 1500 µmol). Therefore, the reagents were weighed into a Duran® glass-ampoule, which was sealed under reduced pressure (p = 1.0 × 10^{-3} mbar) and placed in a tubular-furnace with resistance heating. The ampoule was heated to 210 °C with a heating rate of 10 K·h^{-1}, held at that temperature for 72 h and finally cooled to room temperature with a rate of –10 K·h^{-1}. After the excess pyrazine was separated from the reaction product by sublimation at 120 °C for 12 h, the obtained colorless, crystalline product was characterized by single-crystal- and powder-X-ray diffraction analyses as well as IR spectroscopy. $Sb_2Cl_6(C_4H_4N_2)_3$: calcd. C: 20.69, H: 1.74, N: 12.07 %; found: C: 20.09, H: 1.87, N: 11.77 %. **FT-IR** (ATR): $\tilde{\nu}$ = 3094 (w), 3055 (w), 2979 (w), 2927 (w), 2591 (w), 1473 (m), 1409 (s), 1171 (m), 1157 (m), 1120 (m), 1068 (w), 1029 (s), 794 (s), 777 (s), 762 (s), 723 (w) cm^{-1}.

Synthesis of $^3_\infty[Sb_2I_6(pyz)_3]$ (3): 3 was obtained by a solvent-free melt reaction of 125.6 mg SbI_3 (1 equiv., 250 µmol) with 80.1 mg pyrazine (4 equiv., 1000 µmol). After the reagents were weighed into a Duran® glass-ampoule the ampoule was sealed under reduced pressure (p = 1.0 × 10^{-3} mbar). Subsequently, the ampoule was placed in a tubular-furnace with resistance heating and heated to 100 °C with a heating rate of 20 K·h^{-1}, the temperature was held for 48 h, and the reaction

mixture was finally cooled to room temperature with a rate of –20 K h^{-1}. Excess pyrazine was separated from the reaction product by sublimation at 90 °C for 12 h. Thereby, the crude reaction product formed several crystals ranging from yellow to red in the middle of the ampoule. Of these crystals only those of **3** were suitable for single-crystal-X-ray-diffraction. However, PXRD analysis shows several different crystalline phases. Hence, **3** could not be obtained as phase-pure bulk product, yet.

Supporting Information (see footnote on the first page of this article): Four tables and five figures on crystallographic data, crystal structures, DSC and IR-spectroscopic investigations.

Acknowledgements

We gratefully acknowledge the Fonds der Chemischen Industrie (FCI) for a PhD scholarship for Jens R. Sorg and the Volkswagen Stiftung for support within the project "Molecular materials – bridging magnetism and luminescence" .

Keywords: Coordination polymers / Antimony / Lone-pair / Pyrazine / Melt-synthesis

References

[1] H. Kunkely, A. Paukner, A. Vogler, *Polyhedron* **1989**, *8*, 2937–2939.
[2] J. M. Kisenyi, G. R. Willey, M. G. B. Drew, *J. Chem. Soc., Dalton Trans.* **1985**, 1073–1075.
[3] I. A. Tossidis, C. A. Bolos, G. A. Katsoulos, M. P. Sigalas, C. A. Tsipis, *Z. Anorg. Allg. Chem.* **1988**, *567*, 161–172.
[4] G. C. Pellacani, G. Peyronel, W. Malavasi, L. Menabue, *J. Inorg. Nucl. Chem.* **1977**, *39*, 1855–1857.
[5] S. T. Yuan, S. K. Madan, *Inorg. Chim. Acta* **1972**, *6*, 463–466.
[6] A. C. Fabretti, G. C. Franchini, G. Peyronel, *Inorg. Chim. Acta* **1980**, *42*, 217–222.
[7] P. B. Bertran, S. K. Madan, *J. Inorg. Nucl. Chem.* **1974**, *36*, 983–988.
[8] E. D. L. Piló, A. A. Recio-Despaigne, J. G. Da Silva, I. P. Ferreira, J. A. Takahashi, H. Beraldo, *Polyhedron* **2015**, *97*, 30–38.
[9] H. D. Yin, J. Zhai, *Inorg. Chim. Acta* **2009**, *362*, 339–345.
[10] S. Abdolmaleki, N. Yarmohammadi, H. Adibi, M. Ghadermazi, M. Ashengroph, H. A. Rudbari, G. Bruno, *Polyhedron* **2019**, *159*, 239–250.
[11] A. I. Poddel'sky, M. V. Arsenyev, T. V. Astaf'eva, S. A. Chesnokov, G. K. Fukin, G. A. Abakumov, *J. Organomet. Chem.* **2017**, *835*, 17–24.
[12] S. A. Chesnokov, N. A. Lenshina, M. V. Arsenyev, R. S. Kovylin, M. A. Baten'kin, A. I. Poddel'sky, G. A. Abakumov, *Appl. Organomet. Chem.* **2016**, *30*, e3553.
[13] S. V. Baryshnikova, E. V. Bellan, A. I. Poddel'sky, M. V. Arsenyev, I. V. Smolyaninov, G. K. Fukin, A. V. Piskunov, N. T. Berberova, V. K. Cherkasov, G. A. Abakumov, *Eur. J. Inorg. Chem.* **2016**, 5230–5241.
[14] M. V. Arsen'ev, L. S. Okhlopkova, A. I. Poddel'skii, G. K. Fukin, *Russ. J. Coord. Chem.* **2018**, *44*, 162–168.
[15] A. Koppaka, S. H. Park, B. G. Hashiguchi, N. J. Gunsalus, C. R. King, M. M. Konnick, D. H. Ess, R. A. Periana, *Angew. Chem. Int. Ed.* **2019**, *58*, 2241–2245.
[16] R. N. Duffin, V. L. Blair, L. Kedzierski, P. C. Andrews, *J. Inorg. Biochem.* **2018**, *189*, 151–162.
[17] J. R. Sorg, T. Schneider, L. Wohlfarth, T. C. Schäfer, A. E. Sedykh, K. Müller-Buschbaum, *Dalton Trans.* **2020**, *49*, 4904-4913.
[18] S. Sivasekar, K. Ramalingam, C. Rizzoli, *Polyhedron* **2015**, *85*, 598–606.
[19] H.-X. Qi, H. Jo, H. E. Lee, J. Hong, K. M. Ok, *J. Solid State Chem.* **2019**, *274*, 69–74.
[20] I. Ghesner, L. Opris, G. Balazs, H. J. Breunig, J. E. Drake, A. Silvestru, C. Silvestru, *J. Organomet. Chem.* **2002**, *642*, 113–119.
[21] N. Avarvari, E. Faulques, M. Fourmigué, *Inorg. Chem.* **2001**, *40*, 2570–2577.
[22] R. Ohyama, M. Takahashi, M. Takeda, *Hyperfine Interact.* **2005**, *161*, 99–111.
[23] M. Takeda, M. Takahashi, R. Ohyama, I. Nakai, *Hyperfine Interact.* **1986**, *28*, 741–744.
[24] S. R. Batten, N. R. Champness, X.-M. Chen, J. Garcia-Martinez, S. Kitagawa, L. Öhrström, M. O'Keeffe, M. Paik Suh, J. Reedijk, *Pure Appl. Chem.* **2013**, *85*, 1715–1724.
[25] J.-R. Li, J. Sculley, H.-C. Zhou, *Chem. Rev.* **2012**, *112*, 869–932.
[26] T. A. Makal, J.-R. Li, W. Lu, H.-C. Zhou, *Chem. Soc. Rev.* **2012**, *41*, 7761–7779.
[27] L. J. Murray, M. Dinca, J. R. Long, *Chem. Soc. Rev.* **2009**, *38*, 1294–1314.
[28] M. P. Suh, H. J. Park, T. K. Prasad, D.-W. Lim, *Chem. Rev.* **2012**, *112*, 782–835.
[29] K. Sumida, D. L. Rogow, J. A. Mason, T. M. McDonald, E. D. Bloch, Z. R. Herm, T.-H. Bae, J. R. Long, *Chem. Rev.* **2012**, *112*, 724–781.
[30] Z. Zhang, Y. Zhao, Q. Gong, Z. Li, J. Li, *Chem. Commun.* **2013**, *49*, 653–661.
[31] M. D. Allendorf, C. A. Bauer, R. K. Bhakta, R. J. T. Houk, *Chem. Soc. Rev.* **2009**, *38*, 1330–1352.
[32] Y. Cui, Y. Yue, G. Qian, B. Chen, *Chem. Rev.* **2012**, *112*, 1126–1162.
[33] J. Heine, K. Müller-Buschbaum, *Chem. Soc. Rev.* **2013**, *42*, 9232–9242.
[34] S. H. Zottnick, J. R. Sorg, K. Müller-Buschbaum, C. Fouassier, *Luminescence* in: *Encyclopedia of inorganic and bioinorganic chemistry*, Wiley-VCH, Chichester **2019**.
[35] Z. Hu, B. J. Deibert, J. Li, *Chem. Soc. Rev.* **2014**, *43*, 5815–5840.
[36] L. E. Kreno, K. Leong, O. K. Farha, M. Allendorf, R. P. van Duyne, J. T. Hupp, *Chem. Rev.* **2012**, *112*, 1105–1125.
[37] J. Lei, R. Qian, P. Ling, L. Cui, H. Ju, *TrAC Trends Anal. Chem.* **2014**, *58*, 71–78.
[38] D. Liu, K. Lu, C. Poon, W. Lin, *Inorg. Chem.* **2014**, *53*, 1916–1924.
[39] K. Müller-Buschbaum, F. Beuerle, C. Feldmann, *Microporous Mesoporous Mater.* **2015**, *216*, 171–199.
[40] J. R. Sorg, T. Wehner, P. R. Matthes, R. Sure, S. Grimme, J. Heine, K. Müller-Buschbaum, *Dalton Trans.* **2018**, 7669–7681.
[41] O. Toma, M. Allain, F. Meinardi, A. Forni, C. Botta, N. Mercier, *Angew. Chem. Int. Ed.* **2016**, *55*, 7998–8002.
[42] J. P. H. Charmant, Jahan, A. H. M. Monowar, N. C. Norman, A. G. Orpen, T. J. Podesta, *CrystEngComm* **2004**, *6*, 29.
[43] A. Morsali, *Solid State Sci.* **2006**, *8*, 82–85.
[44] J. R. Sorg, K. C. Oberst, K. Müller-Buschbaum, *Z. Anorg. Allg. Chem.* **2018**, *644*, 1293–1296.
[45] G. E. Gomez, R. F. D'vries, D. F. Lionello, L. M. Aguirre-Díaz, M. Spinosa, C. S. Costa, M. C. Fuertes, R. A. Pizarro, A. M. Kaczmarek, J. Ellena, L. Rozes, M. Iglesias, R. van Deun, C. Sanchez, M. A. Monge, G. J. A. A. Soler-Illia, *Dalton Trans.* **2018**, *47*, 1808–1818.
[46] S. M. F. Vilela, A. A. Babaryk, R. Jaballi, F. Salles, M. E. G. Mosquera, Z. Elaoud, S. van Cleuvenbergen, T. Verbiest, *Eur. J. Inorg. Chem.* **2018**, 2437–2443.
[47] S. Iram, M. Imran, F. Kanwal, Z. Iqbal, F. Deeba, Q. J. Iqbal, *Z. Anorg. Allg. Chem.* **2019**, *645*, 50–56.
[48] J. Heine, T. Wehner, R. Bertermann, A. Steffen, K. Müller-Buschbaum, *Inorg. Chem.* **2014**, *53*, 7197–7203.
[49] A. N. Usoltsev, S. A. Adonin, A. S. Novikov, M. N. Sokolov, V. P. Fedin, *Russ. J. Coord. Chem.* **2020**, *46*, 23–27.
[50] M. Bujak, J. Zaleski, *J. Solid State Chem.* **2004**, *177*, 3202–3211.
[51] H. J. Breunig, M. Denker, E. Lork, *Z. Anorg. Allg. Chem.* **1999**, *625*, 117–120.

[52] M. Lõkov, S. Tshepelevitsh, A. Heering, P. G. Plieger, R. Vianello, I. Leito, *Eur. J. Org. Chem.* **2017**, 4475–4489.
[53] M. Berthelot, C. Laurence, M. Safar, F. Besseau, *J. Chem. Soc., Perkin Trans. 2* **1998**, 283–290.
[54] P. Deokar, D. Leitz, T. H. Stein, M. Vasiliu, D. A. Dixon, K. O. Christe, R. Haiges, *Chem. Eur. J.* **2016**, *22*, 13251–13257.
[55] K. Müller-Buschbaum, A. Zurawski, *Z. Anorg. Allg. Chem.* **2007**, *633*, 2300–2304.
[56] C. C. Quitmann, V. Bezugly, F. R. Wagner, K. Müller-Buschbaum, *Z. Anorg. Allg. Chem.* **2006**, *632*, 1173–1186.
[57] G. Sheldrick, *Acta Crystallogr., Sect. A: Found. Crystallogr.* **2008**, *64*, 112–122.
[58] G. Sheldrick, *Acta Crystallogr., Sect. A: Found. Crystallogr.* **2015**, *71*, 3–8.
[59] G. Sheldrick, *Acta Crystallogr., Sect. C: Cryst. Struct. Commun.* **2015**, *71*, 3–8.
[60] O. V. Dolomanov, L. J. Bourhis, R. J. Gildea, J. A. K. Howard, H. Puschmann, *J. Appl. Crystallogr.* **2009**, *42*, 339–341.
[61] W. Pennington, *J. Appl. Crystallogr.* **1999**, *32*, 1028–1029.

Received: March 27, 2020
Published Online: May 27, 2020

